J Mol Model (2012) 18:4349–4354
DOI 10.1007/s00894-012-1433-0

ORIGINAL PAPER

Solvent effect on cation–π interactions with Al^{3+}

Julen Larrucea

Received: 1 March 2012 / Accepted: 12 April 2012 / Published online: 13 May 2012

Abstract Cation–π interactions are known to be one of the strongest noncovalent forces in the gas phase, but they rarely occur in a fully solvated environment. The present work used two different ab initio molecular dynamics-based approaches to describe the correlation between the strength of the cation–π interactions and the number of water molecules surrounding the cation. Five different complexes between an aluminum cation and different molecules containing aromatic rings were studied, and the degree of hydration of each complex was varied. Results indicated that cation–π interactions vanish when the aluminum cation is surrounded by more than three water molecules. The results also highlighted the influence of –OH ligands on the interaction strength.

Keywords Cation–pi · Aluminum · Aromatic amino acid · CPMD · Blue moon

Introduction

Aluminum is one of the most abundant metals in the Earth's crust. Although no biological role has been found for it, Al^{3+} cation is known to interact with and alter the functions of many enzymes [1], and it is also related to various neurodegenerative diseases [2].

The interaction between the Al^{3+} cation and biomolecules would ideally be studied by investigating a big system, like a protein or peptide, but due to the large size and complexity of such a system, it is necessary to study smaller subsystems of it instead. As amino acids are the building blocks of proteins, the interactions of Al^{3+} with amino acids are evaluated.

Al^{3+} cation can interact in different ways with biomolecules; besides covalent bonding, cation–π interactions [3] are known to be one of the strongest forces present in the gas phase [4]. Cation–π interactions are even reported to be very strong for Na^{+} complexes [4, 5] in water solution, where cations are surrounded by water molecules so a substantial desolvation penalty must be paid to actually bind the cation [6].

Three of the twenty standard amino acids—phenylalanine (Phe), tyroxine (Tyr), and tryptophan (Trp), also known as the aromatic amino acids—have an aromatic ring, and can thus participate in cation–π interactions.

Various Al^{3+}–aromatic amino acid complexes (involving cation–π interactions) undergoing sequential microhydration have been studied [7], and valuable information was obtained about the most stable configurations.

The usual approach used to calculate the binding energy is based on the difference in the total energies of the reactants and products. Thus, for the reaction

$$\text{cation} + \text{ring} \rightleftarrows \text{complex},$$

the binding energy can be calculated as

$$\Delta E = \sum \text{Products} - \sum \text{Reactants}$$
$$= E_{(\text{complex})} - [E_{(\text{ring})} - E_{(\text{cation})}].$$

For more complex reactions involving multiple bond breaking/creation, such as

$$[\text{Cation} + nH_2O] + \text{ring} \rightleftarrows \text{complex} + H_2O,$$

different approaches (such as the blue moon sampling method used in this work) can be employed.

The work described in the present manuscript was performed to determine the strengths of the covalent and

J. Larrucea
Kimika Fakultatea, Euskal Herriko Unibertsitatea and Donostia International Physics Center (DIPC),
P. K. 1072,
20080 Donostia, Basque Country, Spain

J. Larrucea (✉)
Department of Physics, Nanoscience Center,
University of Jyväskylä,
FI-40014 Jyväskylä, Finland
e-mail: julenl@gmail.com

cation–π interactions between the Al^{3+} cation and aromatic amino acids, as well as between the cation and simpler aromatic rings (benzene and phenol), and to elucidate how these depend on the surrounding solvent.

Computational details

All of the calculations were carried out with the density functional theory (DFT)-based CPMD package [8], with the PBE density functional [9], and using Vanderbilt ultrasoft pseudopotentials [10] implemented [11] for CPMD [12]. The simulations were performed according to the Car–Parrinello molecular dynamics method [13], and utilized a thoroughly calibrated set of parameters, including a 30 Ry plane wave cutoff, a fictitious electron mass (μ) of 900 a.m.u., and a time step of 7 a.u. The total temperature of the free system was set at 300 K using the Nose–Hoover thermostat [14–16].

The initial structures of the benzene and phenol complexes were built by hand and relaxed by geometry optimization, while the initial structures used for the aromatic amino acids were the best ones obtained in a previous study [7].

The amount of solvent used in all of the full solvation simulations was 50 water molecules, similar to the number used in previous works [5]. The simulation cell was calculated to be a cube 12.18 Å on a side, and had the same density as bulk water (1 g/cm^3).

Differences in free energy can be measured experimentally based on the probability of finding a system in a given state or the reversible work needed to move from one state to another.

In this work, the binding free energies were calculated in two different ways. Both of them used the distance between C_α and the Al^{3+} cation (atoms highlighted in black and gray, respectively, in Fig. 1) as the reaction coordinate.

The first method is known as thermodynamic integration or "blue moon sampling" [17, 18]. In practice, the procedure was carried out by running an initial unconstrained molecular dynamics simulation for around 3 ps until the system was stable. The distance between the chosen atoms was then constrained, and the average force between these two atoms was calculated using a 3 ps constrained molecular dynamics simulation without a thermostat. After that, the previously mentioned distance was extended (by 0.1 Å in this case), and the average force was calculated again, and this procedure was repeated until the interaction between the atoms vanished. The total interaction energy is defined as the heat and work exchanged by the first law of thermodynamics, but if the systems are adiabatic it can be calculated by simply integrating the average force over the distance:

$$E = \delta Q + \delta W = \delta W = -\int_{r_1}^{r_2} F(r)\, dr.$$

The second method, which utilizes unconstrained molecular dynamics simulations, is based on the probability distribution $P(r)$ [17]. This distribution can be calculated by building a histogram of the reaction coordinate value for each step, and then transforming the resulting values into the free Helmholtz free energy via the relation

$$\Delta F(r) = -R\ T \ln \frac{P(r)}{max(P(r))}.$$

The results obtained in both cases are shown as a graphical representation of $E(r)$ vs r, where r is the reaction coordinate.

Therefore, two different kinds of molecular dynamics simulations were performed: constrained ones for thermodynamic integration, and unconstrained ones for radial distribution functions and to calculate the energy through $P(r)$.

The radial distribution functions [$g(r)$ or g_{XY} for X and Y species] used for the structural analysis and the free energies were calculated using codes written in-house.

Results

Binding of Al^{3+} to benzene and phenol

The stabilities of the cation–π complexes were initially estimated by performing unconstrained molecular dynamics simulations for both benzene (C_6H_6) and phenol (C_6H_5–OH) complexes in a full-solvation environment. In these simulations, the cation–π interactions disappeared in the first few picoseconds, while the Al^{3+} cation was immediately

Fig. 1 Figure showing the C_α carbon (*dark gray*) and Al^{3+} (*light gray*) used for distance monitoring in Phe, Tyr, and Trp, respectively

surrounded by four water molecules. This initial guess established that cation–π interactions involving Al^{3+} in water solution were not present in solution, and as the isolated complexes were highly stable [7], the remaining task was to study the weakening of these interactions under different degrees of hydration.

The trajectories of these simulations were used to calculate their respective radial distribution functions, which provided some interesting reference distances, including r_{OAl} values from 1.74 to 1.8 Å and an r_{CAl} value of 1.5 Å.

After the initial guess, constrained molecular dynamics simulations were performed on the complexes using the blue moon sampling method. The settings for thermodynamic integration were validated because the C_6H_6–Al^{3+} interaction energy of 44.3 kcal/mol obtained from blue moon sampling was similar to those reported in previous studies—an experimental binding energy ($\Delta E = E_{complex} - E_{cation} - E_{ring}$) of 35.2 kcal/mol [19] and a theoretical value of 39.0 kcal/mol (6-31 G(d,p)-MP2 [4]).

We could not find any experimental reference data for the solvated complexes, due to the complexity of the measurements.

The free-energy profiles for cation–π interactions with C_6H_6 and C_6H_5–OH are displayed in Fig. 2 and summarized in Table 1. In the case of C_6H_6, the interaction energy decreases with the number of surrounding water molecules; when this number increases to three, the force needed to pull the cation away from the ring becomes negative in the critical interval. This means that the C_6H_6–Al^{3+} complex should break up when three or more water molecules are present. The case with just a single surrounding water

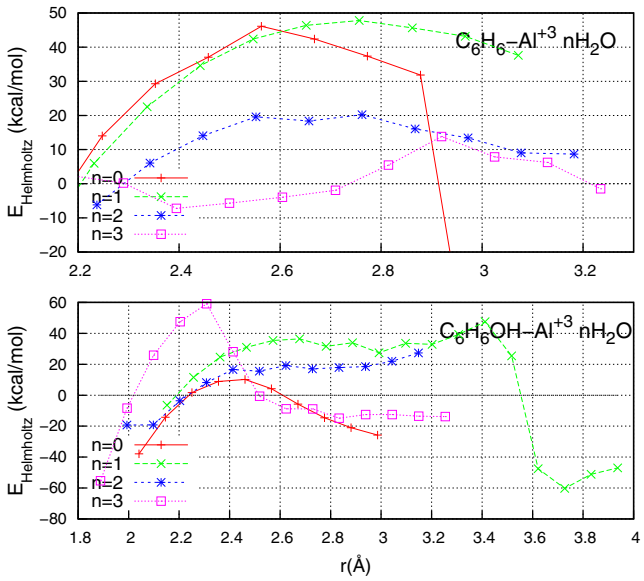

Fig. 2 Free-energy profiles for the cation–π interactions between C_6H_6 or C_6H_6–OH and Al^{3+} with different numbers of surrounding water molecules (energy in kcal/mol)

Table 1 Free energies needed to overcome the cation–π interactions between C_6H_6 and C_6H_5–OH and Al^{3+} with different numbers of surrounding water molecules, as calculated by thermodynamic integration (energies in kcal/mol)

Species complexed with Al^{3+}	nH_2O			
	$n=0$	$n=1$	$n=2$	$n=3$
C_6H_6	44.3	44.4	20.2	13.8
C_6H_5–OH	12.6	37.4	19.2	59.1

molecule yields a very similar interaction energy to the case with no water molecules; the difference between the two values may be due to the lower mobility of the Al^{3+}–H_2O complex with respect to a single Al^{3+} cation, which means that more work is needed to pull them apart.

However, in the case of C_6H_5–OH, the interactions show more complicated behavior than those seen with C_6H_5. The strength of the interaction between the aromatic π electrons from the ring in C_6H_5–OH and Al^{3+} is only 12.6 kcal/mol for the isolated complex, but adding one water molecule leads to a much stronger interaction. Adding another water molecule causes the interaction strength to decrease, but an even stronger interaction than before is seen with three water molecules. An explanation for this phenomenon is provided by the hydrogen bonds between the water molecules and the –OH radical in the C_6H_5–OH.

All of the calculations were performed several times using different parameters and initial configurations, and the energies obtained at the same distance were always comparable (<5 % variation in energy, even with a shorter sampling period).

The cation–π interactions in benzene and phenol occur somewhere in the region Al–C_α=2.2–3.2 Å.

Due to the very different behaviors of the rings, a Mulliken charge analysis was performed. The charge on Al^{3+} was 1.4 e for both systems with one or two water molecules. However, with no water molecules, it was 1.7 and 1.5 e for benzene and phenol, respectively, and it was 1.3 and 1.2 e, respectively, with three water molecules. Therefore, the –OH group in the phenol seems to destabilize π electrons and weaken cation–π interactions.

Complexation with aromatic amino acids

Initial guesses for the different structures were obtained once again by running unconstrained molecular dynamics simulations for Phe, Tyr, and Trp in the same way as done for C_6H_6 and C_6H_5–OH. The initial structures used for the energy calculations were based on the optimum structures (in gas phase) that showed cation–π interactions [7] and were surrounded by water (Fig. 3).

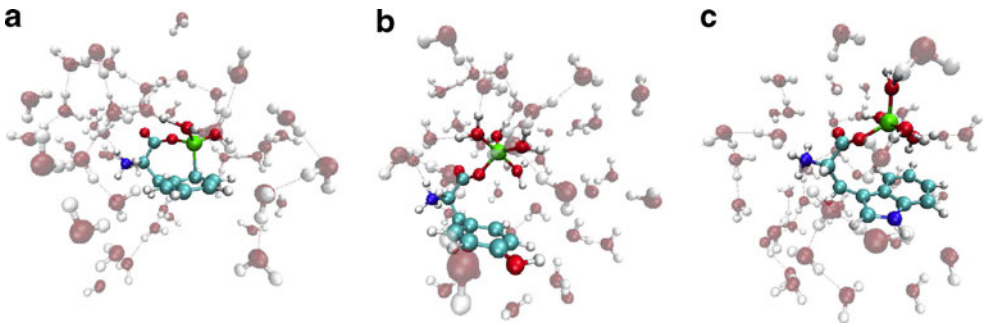

Fig. 3 Snapshots of the simulations of fully solvated ($50H_2O$) complexes with Al^{3+} and Phe, Tyr, or Trp

The cation–π interactions were again lost after a few picoseconds, as the Al^{3+} cation was jettisoned from the aromatic ring and replaced with another water molecule, thus proving the weakness of cation–π interactions in a water solution.

On the other hand, the Al^{3+} cation has been reported to have coordination numbers of 4 and 6 in water solution, and the case with five neighboring water molecules was shown to have the lowest stability [6, 20]. In order to test the coordination of Al^{3+} in complexes, the most stable complexes with Tyr or Trp and five-coordinated Al^{3+} (zw1 and zw2-6 in [7]), surrounded by four water molecules, were simulated in the fully solvated environment (Fig. 3b, c).

The CPMD code intrinsically calculates the electronic structure of the system, and allows the Kohn–Sham orbitals to be transformed into maximally localized Wannier functions and their associated Wannier function centers (WFC) for individual electronic orbitals. The WFCs for the initial structure of Phe are displayed in Fig. 4. There is a WFC at each covalent bond and lone pair in oxygen and nitrogen. Unlocalized π electrons are represented by the WFCs located inside the aromatic ring, and the WFC close to the cation is attracted by the cation, which polarizes the π-electronic density [21], strengthening the interaction.

It is possible to perform an initial guess for the structure of the Al^{3+} cation by considering g_{OAl} displayed in Fig. 5, which shows the influence of the coordination number (n) on the bond strength: the Al–O distances for the $n=3$ coordinated Al^{3+} cation in the Phe simulation and the $n=5$ coordinated Al^{3+} cation in the Tyr and Trp simulations differ by around 0.2 Å. These coordination numbers are lower than that expected for the Al^{3+} cation in water solution [20, 22, 23].

The distances to the first solvation shell around Al^{3+} for these complexes, calculated using various methods and for different environments (microsolvated or in water solution), are summarized in Table 2.

The coordination shells were further from the Al^{3+} cation in water solution (1.9–2.0 Å) than in a microsolvated environment in the gas phase (1.72–1.95 Å) for the same coordination number ($n=5$) [7]. On the other hand, the O–Al distance, 4.0 Å, is less than that measured for Al^{3+} in bulk water (4.14 Å) [6, 24, 25].

The integrals of the radial distribution functions indicated an average coordination number of three for Phe with the first solvation layer (excluding the aromatic ring), and 8–10 with the second layer. For Tyr and Trp, the coordination number with the first solvation layer was five for both, but around twelve for Tyr and eight for Trp with the second layer.

Three different thermodynamic integrations were performed for each amino acid: one for the aromatic amino acid–Al^{3+} isolated complex, one for the complex with two water molecules, and one for the complex in water solution (with 50 water molecules).

The first significant conclusion to be drawn from the results of those calculations is that, once again (see Table 3), the cation–π interaction is much weaker in the presence of solvent. Also, there are much stronger interactions with the aromatic amino acids than with benzene and phenol because the aromatic side chain holds the cation against the ring. It is also noticeable that the cation–π interactions of the unhydrated Tyr and (especially) Trp complexes are stronger than the cation–π interaction of the Phe complex.

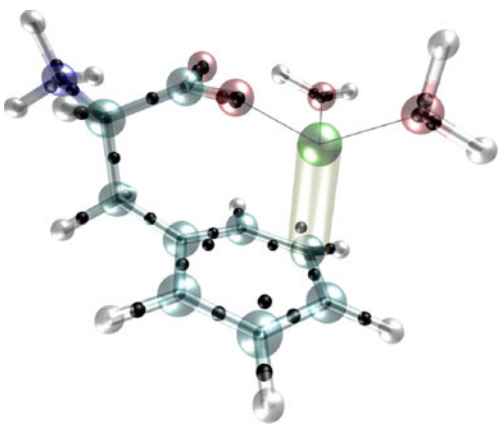

Fig. 4 Maximally localized Wannier function centers (represented by *black spheres*) for the starting configuration of Phe

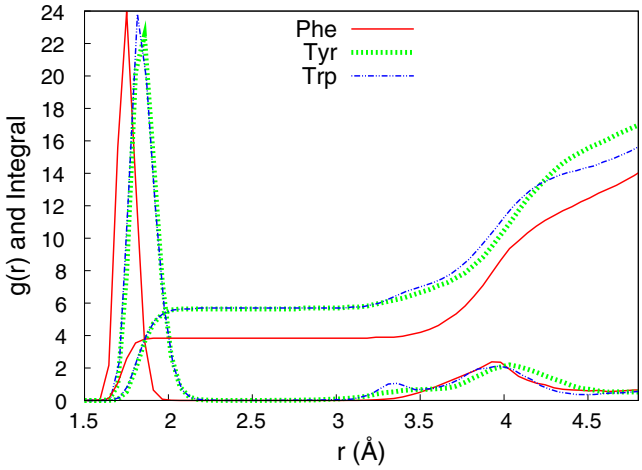

Fig. 5 g_{OAl} and the corresponding integrals for the simulations of the fully solvated ($50H_2O$) complexes with Al^{3+} and Phe, Tyr, or Trp

The energy was also estimated using the probability distribution $P(r)$. Figure 6 displays the results obtained for benzene, phenol, and Phe, where the energy was estimated by calculating the difference between the minima (maximum probability) and the maxima (minimum probability). When a >100 ps molecular dynamics simulation was realized using this approach, the interaction energy for Phe was found to be at least 25 kcal/mol. It is particularly difficult to calculate this barrier using unconstrained molecular dynamics, since (as mentioned before) the Al^{3+} cation does not participate in cation–π interactions in water solution, so the sampling time for the structure with a cation–π interaction is around 1 ps (the rest of the data—around 30 ps—corresponds to a structure where a water molecule has been added to the first solvation layer of the cation and there is no cation–π interaction). Therefore, based on limited data, the cation–π interaction energy for fully solvated benzene is at least 6 kcal/mol, which is in agreement with the value of 13 kcal/mol obtained previously by thermodynamic integration.

Table 2 Comparison of the Al–O distances (in Å) obtained by different methods [single point (SP) and $g(r)$] for four- and five-coordinated Al^{3+} in different environments [microsolvated (MS) and water solution (WS)]. The Gaussian 03 (G03) calculations were performed at the B3LYP/6-31 + G(d,p) level [6]

Method	n=3 (Phe)	n=5 (Tyr / Trp)
SP^{MS}–G03	1.76	1.81 / 1.92
SP^{MS}–PBE	1.76	1.82 / 1.92
$g(r)^{MS}$–PBE	1.87	1.72–1.95
$g(r)^{WS}$–PBE	1.79–1.90	1.9–2.0
$g(r)^{WS}$–PBE	–	1.85

Table 3 Free energies needed to break the cation–π interactions in complexes of Al^{3+} with different amino acids and different amount of surrounding water molecules, as calculated using the blue moon sampling method (energies in kcal/mol)

Amino acid complexed with Al^{3+}	nH_2O		
	n=0	n=2	n=50
Phe	62.6	15.3	37.1
Tyr	98.1	79.1	28.7
Trp	143.2	43.4	40.0

Conclusions

One of the most important conclusions that can be drawn from this study is that interactions involving aromatic π electrons are highly complex. In fact, based on intuition, the binding energies of the complexes should decrease as water molecules are added around the cation, since the charge on the cation is shared with an increasing number of water oxygens, reducing the strength of the electrostatic interaction. However, our highly reproducible results indicate that this is not necessarily true for asymmetric rings (which are all, except benzene). The –OH ligand in the aromatic ring appears to break the symmetry of the π orbital, and the high electronegativity of the oxygen facilitates the creation of H-bonds between the water molecules and Al^{3+}. Overall, this work shows that cation–π interactions with Al^{3+} only occur in isolated gas-phase complexes and complexes surrounded by less than three water molecules.

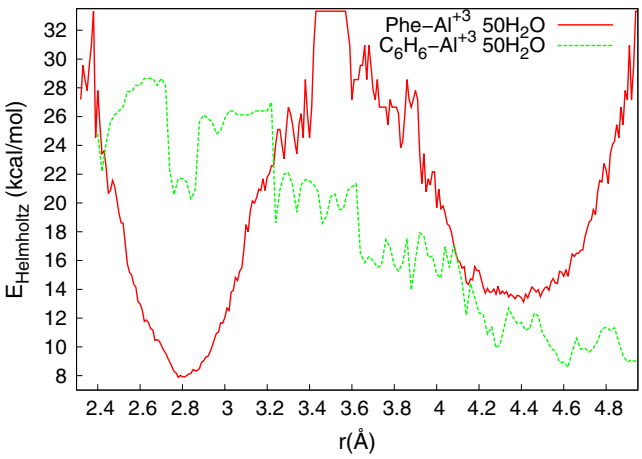

Fig. 6 Free-energy profiles of the cation–π interactions between fully solvated Phe or benzene and Al^{3+}, obtained using the probability distribution $P(r)$; energies are in kcal/mol

Acknowledgments This research was mostly funded by Euskal Herriko Unibertsitatea (the University of the Basque Country), Gipuzkoako Foru Aldundia (the Provincial Government of Gipuzkoa), and Eusko Jaurlaritza (the Basque Government).

The calculations were performed using the Mare Nostrum supercomputer (PowerPC 970MP) at the Barcelona Supercomputing Center (Centro Nacional de Supercomputación), Juropa (Intel Xeon 5570) at the Jülich Supercomputing Center, and Arina (Itanium II) at the SGI/IZO-SGIker at the University of the Basque Country UPV/EHU.

I wish to acknowledge Prof. Jesus M. Ugalde and many people in NSC Jyväskylä, such as Dr. Jaakko Akola, Prof. Hannu Häkkinen, Prof. Robert van Leuwen, and Oleg O. Kit, for discussions and support.

References

1. Zatta P, Lucchini R, van Rensburg SJ, Taylor A (2003) Brain Res Bull 62:15–28
2. Kawahara M (2005) J Alzheim Dis 8:171–181
3. Dougherty DA (1996) Science 271:163–168
4. Ma JC, Dougherty DA (1997) Chem Rev 97:1303–1324
5. Costanzo F, Valle RGDJ (2008) Phys Chem 112:12783–12789
6. Larrucea J (2009) Computational study of the effect of aluminum cation on aromatic amino acids (Ph.D. thesis). Euskal Herriko Unibertsitatea UPV/EHU, Donostia
7. Larrucea J, Rezabal E, Marino T, Russo N, Ugalde JM (2010) J Phys Chem B 114:9017–9022
8. CPMD Consortium (2001) CPMD v3.11.1, C. (revision A11). IBM Corporation/Max-Planck Institut, Stuttgart. http://www.cpmd.org
9. Perdew JP, Burke K, Ernzerhof M (1996) Phys Rev Lett 77:3865–3868
10. Vanderbilt D (1990) Phys Rev B 41:7892–7895
11. Laasonen K, Car R, Lee C, Vanderbilt D (1991) Phys Rev B 43:6796–6799
12. Laasonen K, Pasquarello A, Car R, Lee C, Vanderbilt D (1993) Phys Rev B 47:10142–10153
13. Car R, Parrinello M (1985) Phys Rev Lett 55:2471–2474
14. Nosé SJ (1984) Chem Phys 81:511
15. Hoover WG (1985) Phys Rev A 31:1695
16. Evans DJ, Holian BLJ (1985) Chem Phys 83:4069
17. Sprik M, Ciccotti GJ (1998) Chem Phys 109:7737–7744
18. Ciccotti G, Kaprai R, Vanden-Eijnden E (2006) Chem Phys Chem 6:1809
19. Dunbar RC, Klippenstein SJ, Hrusak J, Stoeckigt D, Schwarz H (1996) J Am Chem Soc 118:5277
20. Larrucea J (2011) Phys Scr 84:045305
21. Suipizi M, Carloni PJ (2000) Phys Chem B 104:10087
22. Swaddle TW, Rosenqvist J, Yu P, Bylaska E, Philips BL, Casey WH (2005) Science 308:1450–1453
23. Takashi Ikeda MH, Kimura TJ (2006) Chem Phys 124: 074503–1
24. Bock CW, Markham GD, Katz AK, Glusker JP (2006) Theor Chem Acc 115:100–112
25. Sillanpää A, Päivärinta JT, Hotokka MJ, Rosenholm JB, Laasonen KJ (2001) Phys Chem 105:10111–10122